

Beyond quasi-particle self-consistent *GW* for molecules with vertex corrections

Arno Förster*

Theoretical Chemistry, Vrije Universiteit Amsterdam, De Boelelaan 1105, 1081 HV Amsterdam, The Netherlands

E-mail: a.t.l.foerster@vu.nl

Abstract

We introduce the $\Sigma^{\text{BSE}@L^{\text{BSE}}}$ self-energy in the quasi-particle self-consistent *GW* (qs*GW*) framework ($\text{qs}\Sigma^{\text{BSE}@L^{\text{BSE}}}$). Here, L is the two-particle response function which we calculate by solving the Bethe-Salpeter equation with the static, first-order *GW* kernel. The same kernel is added to Σ directly. For a set of medium organic molecules, we show that including the vertex both in L and Σ is crucial. This approach retains the good performance of qs*GW* for predicting first ionization potentials and fundamental gaps, while it greatly improves the description of electron affinities. Its good performance places $\text{qs}\Sigma^{\text{BSE}@L^{\text{BSE}}}$ among the best-performing electron propagator methods for charged excitations. Adding the vertex in L only, as commonly done in the solid state community, leads to devastating results for electron affinities and fundamental gaps. We also test the performance of $\text{BSE}@qsGW$ and $\text{qs}\Sigma^{\text{BSE}@L^{\text{BSE}}}$ for neutral charge-transfer excitation and find both methods to perform similar. We conclude that $\Sigma^{\text{BSE}@L^{\text{BSE}}}$ is a promising approximation to the electronic self-energy beyond *GW*. We hope that future research on dynamical vertex effects, second-order vertex corrections, and full self-consistency will improve the accuracy of this method, both for charged and neutral excitation energies.

1 Introduction

The *GW* approximation (GWA) to Hedin’s equations for the electronic self-energy^{1–5} is by now widely used to calculate molecular charged excitation energies.^{6–9} Here, G stands for the single-particle Green’s function, and W is the dynamically screened Coulomb interaction typically calculated within the random phase approximation (RPA).^{10,11} The GWA approximates the exchange-correlation self-energy of a many-body system by adding correlation in the form of dynamical screening [typically calculated within the random phase approximation (RPA)]^{10,12} to the bare Fock exchange.⁶

Since G and W depend on the knowledge of G itself, the GWA defines a self-consistent set of equations. During the self-consistent optimization of the interacting G , spectral weight, measured by the quasi-particle (QP) renormalization factor Z , is transferred from the QP peak to satellite features.^{13,14} Consequently, the GWA underestimates the polarization due to particle-hole excitations and therefore severely underestimates the screening of the electron interaction.¹⁴ In practice, this leads to overestimated QP energies and gaps, and a poor description of satellites.^{15–19}

Replacing the interacting G with an effective $G^{(0)}$, typically obtained from a Kohn–Sham (KS)²⁰ calculation, and treating the *GW* self-energy as a perturbation offers a simple solution to this problem.²¹ Since $Z = 1$ by definition, the under-screening problem is avoided. Careful selection of the KS starting point results in more accurate molecular QP energies at lower cost.^{22–28} However, this so-called G_0W_0 approach introduces an undesirable dependence on the KS reference.^{22,26,29–32} An iterative update of the G_0W_0 eigenvalues largely removes the starting-point dependence for charged excitations,²⁹ but not for optical excitations from the *GW*-Bethe-Salpeter equation (BSE) method.^{2,33–35}

Quasi-particle self-consistent *GW* (qs*GW*)^{13,36,37} addresses this starting-point dependence by replacing the Dyson equation for G by an effective single-particle problem, obtained through Hermitization of the self-energy. By self-consistent optimization of the effective single-particle Hamiltonian, one finds an optimal $G^{(0)}$ within the GWA.¹⁴ The self-consistency condition rigorously removes the dependence on the DFT starting point³⁸ for charged and optical excitations.^{39–41} qs*GW*

has been applied first to solids^{13,36,37,42,43} where it performs somewhat better than *scGW* but still overestimates the band gaps of solids by about 10-20%.^{36,42,44-46}

This issue can be addressed by including higher-order diagrams in the self-energy through so-called vertex corrections which describe the scattering between particle-hole pairs. The vertex enters the self-energy Σ directly, but also through the response function L which in Hedin's equations determines W .⁵ Within *qsGW*, vertex corrections have been predominantly considered in L only, but not in the self-energy.^{42,44,46,47} The reasons for this are two-fold. First, vertex-corrections in L , be it through approximate exchange-correlation kernels^{42,44} or the non-local first-order vertex in Hedin's equations,^{46,47} account for the electron-hole interaction missing in the RPA and therefore close the band gap, while corrections in the self-energy are known to open the gap.^{26,48} The second argument relies on the Ward identity which states that the vertex function Γ goes as $1/Z$ in the long-range and zero-frequency limit.⁴⁹ Since in the exact self-energy $\Sigma = iGW\Gamma$ the Z -factors in G , which renormalizes G^0 , and Γ should cancel,^{17,50} Kotani, van Schilfgaarde and Faleev argued that vertex corrections in Σ should be avoided whenever G is replaced by $G^{(0)}$.³⁷ Pasquarello and coworkers argued that this argument only applies in the long-range and in addition to the full vertex in L , introduced a short-range vertex to the self-energy⁴⁵ which they found to have a small effect on band gaps but to improve QP energies.^{45,51}

qsGW has also been used for atoms⁵² and molecules.^{39,53,54} It gives relatively accurate ionization potentials^{23,55,56} and its fundamental gaps are in excellent agreement with Δ -Coupled cluster with single, double and perturbative triple substitutions [Δ CCSD(T)]⁵⁷ for the ACC24 of 24 organic acceptor molecules²² relevant for photovoltaic applications.⁴¹ Interestingly, *qsGW* tends to underestimate these systems' fundamental gaps⁴¹ and the inclusion of a vertex correction in L but not in Σ can only be expected to worsen them. Vertex corrections in L only have been tried in molecular G_0W_0 calculations with HF starting points. While they often improve first ionization potentials (IP),^{24,58,59} they also produce major outliers in benchmarks and are therefore unreliable.

Only a few vertex-corrected *qsGW* calculations have been performed for molecules, and only vertex corrections in the self-energy have been tried.^{26,41,60} These calculations either follow Grüneis

et al.⁴⁸ and perturbatively correct the qsGW QP energies using a statically screened version^{41,48} of the $G3W2$ self-energy,^{17,26} or use the fully dynamical $G3W2$ correction to GW .²⁶ In all cases, no clear improvements over qsGW could be observed. This is not surprising since perturbative vertex corrections to the self-energy^{26,41,61,62} are a bad strategy in molecular G_0W_0 calculations, and can only work if a qualitatively incorrect $G^{(0)}$ is used as a starting point.²⁶ Since qsGW is already relatively accurate, no clear improvements can be expected. Only the statically screened $G3W2$ correction retains the good performance of qsGW, but only because its magnitude is small.⁴¹

Starting from a Hartree-Fock (HF) Green's function, solving the time-dependent HF equations for L , and using the same vertex in Σ in G_0W_0 has been a much more successful strategy.^{59,63–69} This scheme performs well for the calculation of first ionization potentials (IP) of atoms,⁶⁷ smaller molecules in the GW100 set⁵⁹ and also larger systems like linear acenes⁶⁵ and others.⁶⁸ Patterson [using the Tam-Dancoff approximation (TDA)]^{68,69} and Förster, and Bruneval⁵⁹ additionally replaced the bare exchange in the HF equations with statically screened exchange. This replacement is crucial for realistic charged excitations in larger systems where screening effects are important.⁵⁹

Here, we use the same self-energy in molecular qsGW calculations and report benchmark results for IPs, EAs, and fundamental gaps for the ACC24 set. Since we solve the BSE with the screened exchange vertex self-consistently and not only after the GW calculation, we also investigate how the neutral (singlet) excitation energies compare to the ones obtained from standard BSE@qsGW for the QUEST #6 subset⁷⁰ of charge-transfer excitations (CT) of the QUEST database.^{71–73} In section 2, we introduce our expression for the self-energy and discuss differences to the closely related method of Cunningham et al.⁴⁶ In section 3 we present and discuss our numerical results and conclude this work in section 4.

2 Theory

The exact self-energy of an interacting many-electron system can be obtained by solving the following set of coupled equations self-consistently:

$$\begin{aligned}\Sigma_{xc}(1,2) = & iv(1^+,2)G(1,2) \\ & + iv(1^+,3)G(1,4)I(4,6,2,5)L(5,3,6,3)\end{aligned}\quad (1)$$

$$\begin{aligned}L(1,2,3,4) = & L^{(0)}(1,2,3,4) \\ & + L^{(0)}(1,5,3,6)I(6,7,5,8)L(8,2,7,4)\end{aligned}\quad (2)$$

$$G(1,2) = G^{(0)}(1,2) + G(1,4)\Sigma_{xc}(3,4)G(4,2) . \quad (3)$$

Equation (1) combines the 2-point Coulomb interaction v , the 2-particle correlation function L , the single-particle Green's function G , and the kernel

$$I(1,2,3,4) = \delta(1,3)\delta(2,4)v(1,4) + i\frac{\delta\Sigma_{xc}(1,3)}{\delta G(4,2)} . \quad (4)$$

The same kernel also appears in the Bethe-Salpeter equation (BSE) eq. (2) for L , where $L^{(0)}(1,2,3,4) = -iG(1,4)G(2,3)$ is the non-interacting 2-particle correlation function. Integration over repeated indices is implied and integers $n = (\mathbf{r}_n, \sigma_n, t_n)$ collect spatial coordinates, spin, and time. The same or slightly similar sets of equations are known at least since the work of Baym and Kadanoff⁷⁴ and are frequently encountered in the literature.^{5,59,63,67,68,75,76} They are completely equivalent to Hedin's equations.^{2,63,77}

2.1 quasi-particle self-consistent GW

In this work, we solve this set of equations in the qsGW approximation. The aim of a qsGW calculation^{13,14,36,37} is to find an effective $G^{(0)}$ which approximates the interacting G in eq. (3).³⁷ Assuming the self-energy is constant in the vicinity of some reference QP energy ε_p , we rewrite

eq. (3) as

$$\sum_q [\Sigma_{pq}(\varepsilon_p) + \varepsilon_p \delta_{pq}] \phi_q = \omega \phi_p . \quad (5)$$

To get an effective $G^{(0)}$, the self-energy has to be mapped to an effective Hermitian QP Hamiltonian. Different mappings have been proposed^{13,37,42,49,55,78,79} and we follow Ref. 37 and set

$$H_{pq} = \frac{1}{2} \left\{ \text{Re} \Sigma_{pq}(\varepsilon_p^{QP}) + \text{Re} \Sigma_{pq}(\varepsilon_q^{QP}) \right\} . \quad (6)$$

This construction of the QP Hamiltonian has been shown to satisfy a variational principle.⁸⁰ For reasons of numerical stability, a closely related construction¹³ which evaluates the off-diagonal elements of \hat{H}^{QP} at the Fermi-level instead is often preferred in implementations which evaluate Σ by analytical continuation.^{39,81,82} Comparisons between different QP Hamiltonians show that they typically give similar QP energies.^{39,55} This also includes linearized qsGW where the self-energy is Taylor-expanded around the chemical potential and the linear term is retained.^{42,49,79,82} In conclusion, we expect all of our findings to be also valid for other QP Hamiltonians.

2.2 Vertex-corrections in quasi-particle self-consistent GW

Equations (1), (2) and (5) form a closed set of equations. In each iteration, diagonalization of eq. (5) yields a set of molecular orbitals ϕ_p and QP energies ε_p from which the non-interacting $G^{(0)}$ is constructed:

$$G^{(0)}(\mathbf{r}, \mathbf{r}', \omega) = \sum_i^{\text{occ}} \frac{\phi_i(\mathbf{r}) \phi_i(\mathbf{r}')}{\omega - \varepsilon_i - i\eta} + \sum_a^{\text{virt}} \frac{\phi_a(\mathbf{r}) \phi_a(\mathbf{r}')}{\omega - \varepsilon_a + i\eta} . \quad (7)$$

We now approximate the kernel eq. (4) as

$$I(1, 2, 3, 4) = \delta(1, 3) \delta(2, 4) v(1, 4) - \delta(1, 4) \delta(3, 2) W_0(1, 3) , \quad (8)$$

where W_0 is the statically screened Coulomb interaction in the random phase approximation (RPA). Formally, (8) is obtained by making the GWA to the self-energy in (4), neglecting the variation of the dynamical W with respect to G and taking the static limit. With eqs. (7) and (8), eq. (2) becomes a function of a single frequency and can be solved exactly by diagonalization in the particle-hole representation. In the usual notation, eq. (2) becomes⁸³

$$\begin{pmatrix} A & B \\ B & A \end{pmatrix} \begin{pmatrix} X \\ Y \end{pmatrix} = \begin{pmatrix} \Omega & 0 \\ 0 & -\Omega \end{pmatrix} \begin{pmatrix} X \\ Y \end{pmatrix} \quad (9)$$

with the matrix elements

$$\begin{aligned} A_{ia,jb} &= -\delta_{ij}\delta_{ab}(\epsilon_a - \epsilon_i) + (ia|v|jb) - (ij|W_0|ab) \\ B_{ia,jb} &= -\delta_{ij}\delta_{ab}(\epsilon_a - \epsilon_i) + (ia|v|jb) - (ib|W_0|ja) \end{aligned} \quad (10)$$

and chemists' notation for the 2-electron integrals,

$$(pq|K|rs) = \int d\mathbf{r} \int d\mathbf{r}' \phi_p^*(\mathbf{r})\phi_q(\mathbf{r})K(\mathbf{r},\mathbf{r}')\phi_r^*(\mathbf{r}')\phi_s(\mathbf{r}') . \quad (11)$$

Ω is a diagonal matrix containing the system's neutral excitation energies. Solving only for the particle-hole part constitutes no additional approximation beyond the approximation to the kernel eq. (8). While L generally also includes particle-particle and hole-hole terms, these contributions are eliminated when the kernel I is static.⁸⁴ In the basis of molecular orbitals which diagonalize eq. (5), the correlation part of the self-energy eq. (1) with the very same kernel eq. (8) can then be shown to be^{59,67}

$$\Sigma_{pq}(\omega) = \Sigma_{pq}^<(\omega) + \Sigma_{pq}^>(\omega) \quad (12)$$

with

$$\begin{aligned} \Sigma_{pq}^<(\omega) = & \sum_S \sum_k \frac{1}{\omega - \varepsilon_k + \Omega_S - i\eta} \\ & \times \left[\sum_{ia} 2(ai|v|qk)(X_{ia}^S + Y_{ia}^S) - (ka|W_0|qi)X_{ia}^S - (ki|W_0|qa)Y_{ia}^S \right] \\ & \times \left[\sum_{jb} (bj|v|pk)(X_{jb}^S + Y_{jb}^S) \right] \end{aligned} \quad (13)$$

and

$$\begin{aligned} \Sigma_{pq}^>(\omega) = & \sum_S \sum_c \frac{1}{\omega - \varepsilon_c - \Omega_S + i\eta} \\ & \times \left[\sum_{ia} 2(ai|v|qc)(X_{ia}^S + Y_{ia}^S) - (ci|W_0|qa)X_{ia}^S - (ca|W_0|qi)Y_{ia}^S \right] \\ & \times \left[\sum_{jb} (bj|v|pc)(X_{jb}^S + Y_{jb}^S) \right]. \end{aligned} \quad (14)$$

We start our vertex-corrected qsGW calculations from a Hartree-Fock reference. We then solve the RPA equations using the HF $G^{(0)}$ to obtain W_0 which we use to solve eq. (9). Afterward, the self-energy eq. (12) is constructed and used in eq. (6). We then diagonalize eq. (5) to obtain a new set of orbitals ϕ_k and QP energies ε_k and construct the corresponding $G^{(0)}$ eq. (7). This process is iterated until convergence.

following our recent work,⁵⁹ we refer to the self-energy in eqs. (12) to (14) as $\Sigma^{BSE}@L^{BSE}$. For $W_0 = 0$, eq. (12) reduces to the GWA with BSE screening ($GW@L^{BSE}$), and for $W_0 = 0$ also in eq. (10), to the GWA. The former variant has been coined qsG \hat{W} by Cunningham *et. al.*^{46,47} and been applied to a variety of materials.^{85–89} They solved eq. (9) within the TDA⁹⁰ which has later been shown to be a rather severe approximation.⁹¹ The qsG \hat{W} of Cunningham *et. al.*^{46,47} should not be confused with the qsG \hat{W} method of Tal, Chen, and Pasquarello⁴⁵.

Our work extends the method by Cunningham *et al.*⁴⁶ in two important aspects. First, we do not make the TDA in the solution of the BSE [which would correspond to $\mathbf{B} = 0$ in eq. (9)]. Second, and more importantly, we include the very same kernel as in eq. (9) also in the self-energy. Due to its Dyson-like structure, the BSE with the matrix elements eq. (10) generates particle-hole ladder diagrams and resums them to all orders. They describe the electron-hole attraction missing in the

RPA and therefore close the band gap.⁴⁶ This is not desired in molecular *qsGW* calculations since band gaps are already underestimated.⁴¹ As shown in ref. 59, vertex corrections in the self-energy come with an opposite sign and are needed to balance the vertex correction in the screening.

2.3 Computational Details

We performed vertex-corrected *qsGW* calculations with a development version of the BAND engine⁹² of the Amsterdam modeling suite (AMS2024), using the analytical frequency integration expression for the self-energy following Refs. 93 and 55. We have performed all calculations with augmented Dunning basis sets of DZ to QZ quality (aug-cc-pVDZ to aug-cc-pVQZ).^{94,95} We discuss the basis set requirements of all calculations below.

All 4-center integrals are calculated using the pair-atomic density fitting scheme as presented in Ref. 96. The size of the auxiliary basis in this approach can be tuned by a single threshold which we set to $\epsilon_{aux} = 1 \times 10^{-10}$ in all calculations if not stated otherwise. We further artificially enlarge the auxiliary basis by setting the BoostL option.⁹⁶ We further eliminate almost linear dependent products of basis functions from the primary basis by setting the *K*-matrix regularization parameter to 5×10^{-4} .⁹⁶

Since BAND does not support molecular point group symmetry, we calculated neutral excitations with the ADF engine.^{34,97} For the QUEST #6 database of molecular CT excitations⁷⁰ we used STO basis sets ranging from TZP and TZ2P⁹⁸ to TZ3P.⁹⁹ The latter is comparable to cc-pVTZ. Since we use reference values obtained with the cc-pVTZ basis set,⁷⁰ the remaining basis set error should be negligible as well. We verified this by performing additional cc-pVTZ calculations with the BAND code for cases where the correct symmetry of the excitation can easily be verified (see SI for details).

To converge the *qsGW* and *qs* Σ^{BSE} calculations for the ACC24 set, we use a linear mixing strategy,⁶⁰ in which we construct the QP Hamiltonian in (6) for the *n*th iteration as $H^{(n)} \leftarrow \alpha^{(n)}H^{(n)} + (1 - \alpha^{(n)})H^{(n-1)}$. We start the self-consistency field (SCF) cycle with $\alpha^{(0)} = 0.3$. In case the SCF error decreases, we use the mixing parameter $\alpha^{(n)} = \max \left\{ 1.2 \times \alpha^{(n-1)}, 0.5 \right\}$ in the

n th iteration. In case the SCF error increases, we reset the mixing parameter to $\alpha^{(0)}$. We terminate the calculation when the change in the fundamental gap between 2 subsequent iterations is smaller than 1 meV. For reasons of computational efficiency, for the molecules in the QUEST #6 database we use the direct inversion of the iterative subspace (DIIS)¹⁰⁰ algorithm of Ref. 39 (which is based on Ref. 101) with a maximum of 8 iterations.

3 Results

3.1 Charged excitations

3.1.1 Basis set dependence

The slow convergence of individual *GW* QP energies to the complete basis set (CBS) limit in Gaussian basis sets is well-documented.^{31,52,53,102} It is however rarely emphasized that *GW* QP energies converge slower to the basis set limit than the ones calculated with CC methods which are often used for benchmarking *GW*, like Δ CCSD(T) or equation-of-motion (EOM)-CC^{103–105} methods. These different convergence rates imply that comparison to CC reference values should ideally be performed in a large basis set to eliminate basis set errors. Alternatively, the basis set limit may be estimated by extrapolation which requires performing at least a QZ calculation for a relatively precise estimate.¹⁰⁶ As a rule of thumb, the extrapolated result will be roughly of 5Z quality.¹⁰⁷ Since GTO-type basis sets do not converge uniformly to the complete basis set limit such techniques are not ideally suited for precise benchmarks.

In the case of the ACC24 benchmark, Richard et al.¹⁰⁸ report basis set limit extrapolated first IPs and EAs. The extrapolated values are always obtained by performing a Δ CCSD(T) calculation using a series of calculations with aug-cc basis sets ranging from DZ to QZ quality. The remaining basis set error is estimated by extrapolation with the help of Δ MP2 calculations in larger bases. However, for only 6 out of the 24 systems in their set, they performed a Δ CCSD(T)/aug-cc-pvQZ calculation and for 4 of them, they only reported Δ CCSD(T)/aug-cc-pvDZ calculations.

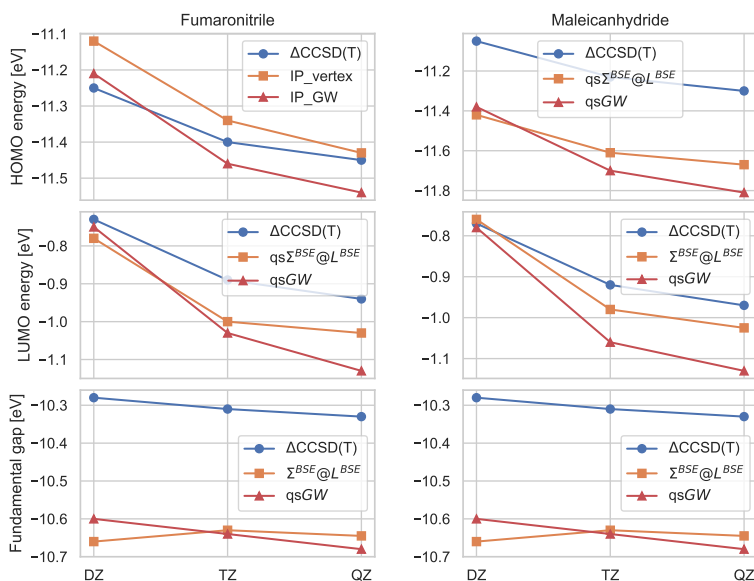


Figure 1: convergence of the HOMO energies (top), LUMO energies (middle), and fundamental gaps (bottom) of Fumaronitrile (left) and Maleic anhydride (right) with respect to the basis set (aug-cc-pVDZ to aug-cc-pVQZ) for $\Delta\text{CCSD(T)}^{108}$, qsGW and $\text{qs}\Sigma^{BSE}@L^{BSE}$. All values are in eV

In the following benchmarks, we prefer to use the pure $\Delta\text{CCSD(T)}$ values as reference, and for a reliable comparison, we first investigate how $\Sigma^{BSE}@L^{BSE}$ converge to the CBS limit, and how this convergence compares to $\Delta\text{CCSD(T)}$. HOMO energies, LUMO energies, and fundamental gaps of Maleic anhydride and Fumaronitrile calculated with all three methods using aug-cc-pVDZ to aug-cc-pVQZ are shown in Fig. 1.

The convergence of the HOMO energy is shown in the upper plot. $\Delta\text{CCSD(T)}$ converges to the CBS limit faster than $\text{qs}\Sigma^{BSE}@L^{BSE}$ and qsGW which show a similar rate of convergence. The LUMO energy of Fumaronitrile and the HOMO and LUMO energies of Maleic anhydride, converge much faster to the CBS limit with $\text{qs}\Sigma^{BSE}@L^{BSE}$ than with qsGW , almost as fast as with $\Delta\text{CCSD(T)}$. Comparing the LUMO energies obtained with different basis sets is particularly insightful. For Fumaronitrile and Maleic anhydride, the $\text{qs}\Sigma^{BSE}@L^{BSE}$ and qsGW LUMO energies agree with $\Delta\text{CCSD(T)}$ within a few ten meV. However, this is partially an artifact of the non-converged basis set. At the QZ level, the difference in the qsGW and $\Delta\text{CCSD(T)}$ LUMO energies

is about 200 meV for Fumaronitririle and 150 meV for Maleic anhydride. The agreement between $qs\Sigma^{BSE}@L^{BSE}$ and $\Delta CCSD(T)$ remains better also for the larger basis sets. The difference in the LUMO energy of Fumaronitririle is 50 meV for DZ and 90 meV for QZ, and for Maleic anhydride the differences are 10 meV and 40 meV, respectively. We also notice that the QP gap between HOMO and LUMO is already converged sufficiently at the DZ level since the basis set errors for HOMO and LUMO are typically the same when augmented GTO basis sets are used.²⁹

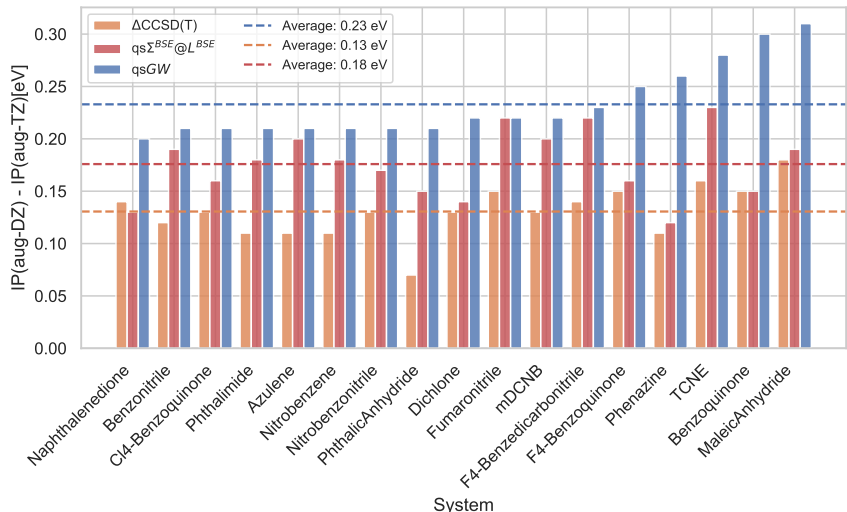


Figure 2: Difference in first IPs in eV calculated with the aug-cc-pVDZ and aug-cc-pVTZ basis sets for $\Delta CCSD(T)$ ¹⁰⁸, $qsGW$ and $qs\Sigma^{BSE}@L^{BSE}$.

Fig. 2 shows the difference between the aug-cc-pVDZ and aug-cc-pVTZ first IPs for a subset of ACC24 for $\Delta CCSD(T)$, $qsGW$ and $qs\Sigma^{BSE}@L^{BSE}$. For $\Delta CCSD(T)$, the average difference in IPs obtained with both basis sets is 0.13 eV, while for $qsGW$, with 0.23 eV this difference is significantly larger. With 0.18 eV on average, $qs\Sigma^{BSE}@L^{BSE}$ converges to the CBS limit faster, not much slower than $\Delta CCSD(T)$. The slow convergence of GW to the CBS limit is due to the absence of exchange terms in the correlation part of the self-energy which converge to the CBS limit with opposite signs than the direct ones.^{26,109} Therefore, the vertex-corrections in $qs\Sigma^{BSE}@L^{BSE}$ lead to faster basis set convergence.

The results of this subsection clearly show that care should be taken when GW results are compared to high-level wave function-based methods in a small basis set. Comparing $qsGW$ to

$\Delta\text{CCSD(T)}$ in a DZ basis set will give a skewed picture of its accuracy. For our present study, we conclude that already at the DZ level $\text{qs}\Sigma^{BSE}@L^{BSE}$ can be faithfully compared to $\Delta\text{CCSD(T)}$, and at the TZ level the basis set error should essentially play no role. The situation is different for qsGW , where a comparison at the DZ level will come with major basis set errors, and calculations of at least TZ level are necessary to assess its performance reliably.

Therefore, all qsGW QP energies shown in the following are obtained with the aug-cc-pVTZ basis set. The same holds for $\text{qs}\Sigma^{BSE}@L^{BSE}$, except for six molecules where we were not able to perform $\text{qs}\Sigma^{BSE}@L^{BSE}/\text{aug-cc-pVTZ}$ calculations due to high memory demands. In these cases, we corrected the IPs and EAs with the average basis set errors of 0.18 eV shown in figure 2. The error of this estimate should be smaller than 50 meV. The IPs and EAs of the 4 systems for which no aug-cc-pVTZ reference values are available are shifted by the ΔMP2 values from Ref. 108. The same has been done for Dinitrobenzotrile, where the aug-cc-pVTZ reference value seems to be incorrectly reported. This correction allows for a fair assessment of the method’s accuracy for the complete ACC24 set. All individual QP energies are listed in the supporting information.

3.1.2 Compensation of vertex corrections in L and Σ

Before comparing the (vertex-corrected) qsGW calculations to $\Delta\text{CCSD(T)}$, we show the effect of the individual vertex corrections in L and Σ in Fig. 3. The orange bars show the magnitude of the vertex correction beyond RPA in L (corresponding to the green dots in Fig. 4) and the blue bars the magnitude of the vertex correction in Σ beyond GW (corresponding to the blue dots in Fig. 4). The red boxes are the blue and orange bars’ sums, showing the difference between $\text{GW}@RPA$ and $\Sigma^{BSE}@L^{BSE}$. As observed previously,⁵⁹ the vertex corrections in Σ and L largely compensate for the HOMO. However, they substantially increase the LUMO (for which the magnitudes of the vertices in L and Σ are also much larger), widening the qsGW HOMO-LUMO gap. This has also been observed by Grüneis et al.⁴⁸ This is likely an artifact of the static vertex. Accounting for the dynamics of the vertex (at least within scGW) should close the fundamental gap.¹⁷

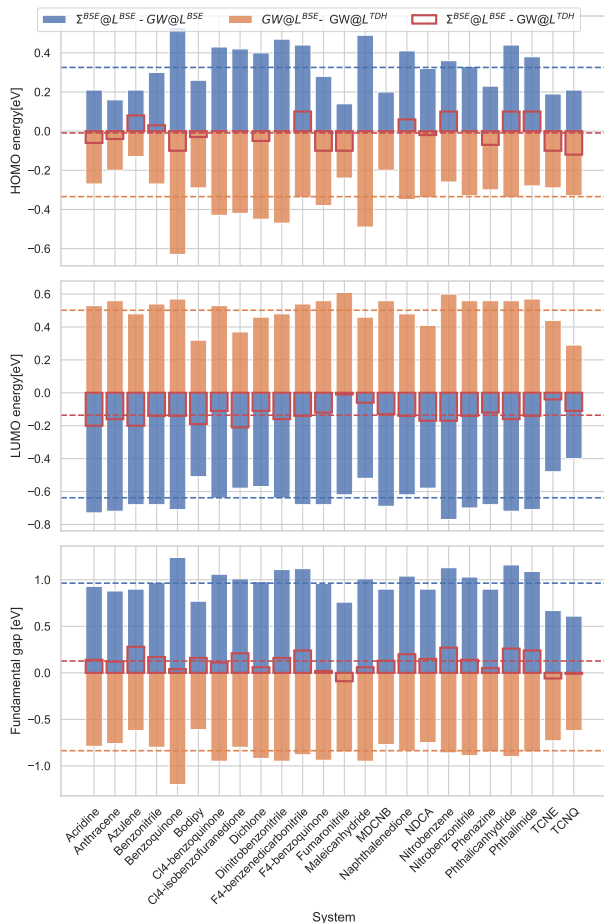


Figure 3: Vertex corrections in eV of the HOMO (top), LUMO (middle), and HOMO-LUMO gap (bottom) of the molecules in the ACC24.

3.1.3 Accuracy of vertex-corrected qsGW

After discussing the basis set errors of the different approximations, we are in a position to compare $qsGW@RPA$, $qsGW@L^{BSE}$ and $qs\Sigma^{BSE}@L^{BSE}$ against the $\Delta CCSD(T)$ reference values from Richard et al.¹⁰⁸ for the ACC24 set. Fig. 4 plots the IPs, EAs, and fundamental gaps obtained with all three MBPT approximations against $\Delta CCSD(T)$. In the supporting information, we show the same plot, but with all values calculated with the aug-cc-pVDZ basis set. Comparing both plots shows, that a benchmark using aug-cc-pVDZ would lead to a skewed picture of the respective methods' accuracy.

We first discuss the IPs. As can be seen from the upper panel in Fig. 3, the vertex corrections in L and Σ in $qs\Sigma^{BSE}@L^{BSE}$ cancel almost completely. Therefore, the differences between

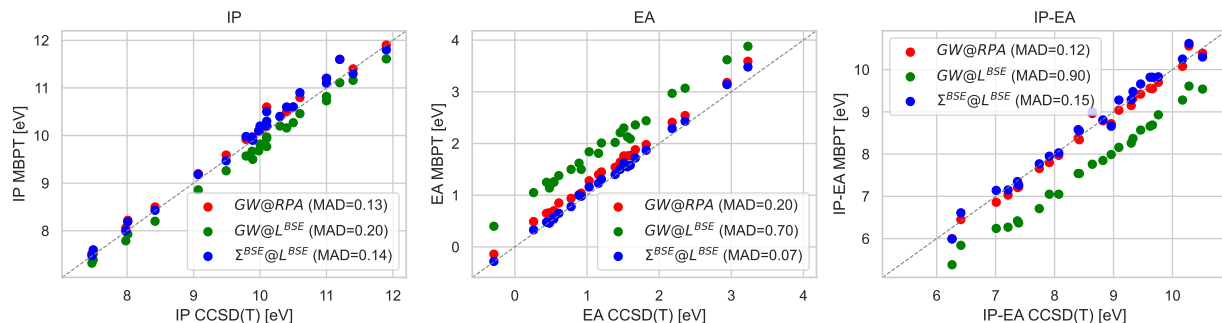


Figure 4: Deviations of the molecules in the ACC24 set to $\Delta\text{CCSD(T)}$ for quasi-particle self-consistent GW@RPA , GW@L^{BSE} and $\Sigma^{BSE}@L^{BSE}$ for IPs (left), EAs (middle) and fundamental gaps (right). All values are in eV.

the $\text{qs}\Sigma^{BSE}@L^{BSE}$ and qsGW@RPA IPs are small. Consequently, with MADs of 0.13 and 0.14 eV, respectively the accuracy of both methods in predicting IPs is very similar. For EAs, the vertex in L dominates the vertex in Σ and therefore the $\text{qs}\Sigma^{BSE}@L^{BSE}$ EAs are much lower than the qsGW@RPA ones. As shown in the middle plot in Fig. 4, this massively improves the agreement with the $\Delta\text{CCSD(T)}$ reference values. $\text{qs}\Sigma^{BSE}@L^{BSE}$ gives an excellent MAD of 0.07 eV, while with 0.20 eV, qsGW@RPA performs significantly worse. Consequently, $\text{qs}\Sigma^{BSE}@L^{BSE}$ gives much larger fundamental gaps than qsGW@RPA . qsGW@RPA underestimates the $\Delta\text{CCSD(T)}$ gaps, but $\text{qs}\Sigma^{BSE}@L^{BSE}$ tends to overcorrect them. In the end, with 0.12 and 0.15 eV, respectively, both methods offer very similar accuracy. Finally, we also comment on the performance of qsGW@L^{BSE} . The IPs are of surprisingly good quality. However, as already anticipated, due to the missing vertex correction in Σ , qsGW@L^{BSE} overestimates EAs, and therefore massively underestimates band gaps.

In Ref. 41 we have already performed qsGW@RPA calculations for the ACC24 set and obtained MADs for IPs, EAs, and fundamental gaps as 0.09 eV, 0.14 eV, and 0.13 eV. In Ref. 41 we have obtained all results by extrapolating the QP energies to the CBS limit using STO-type basis sets of TZ and QZ quality and used the $\Delta\text{CCSD(T)}/\text{CBS}$ values of Ref. 108. Therefore, we must dampen our positive conclusions on the high accuracy of qsGW@RPA a bit. Here, we find the performance of qsGW@RPA to be slightly worse for IPs and EAs, but its performance for fundamental gaps is still excellent.

Table 1: MADs in eV for the ACC24 set for IPs, EAs, and fundamental gaps obtained with different accurate methods.

Method	MAD [IP]	MAD [EA]	MAD [gap]	Reference
qsGW@RPA	0.13	0.20	0.12	This work
qs Σ^{BSE} @ L^{BSE}	0.14	0.07	0.15	This work
G_0W_0 @LRC- ω PBE	0.13	0.18		Ref. 22
G_0W_0 @LC- ω PBE (tuned)	0.09	0.13	0.13	Ref. 110
G_0W_0 @OTRSH	0.09	0.07	0.14	Ref. 26
ADC(3)	0.12	0.16		Ref. 111
ω LH22t	0.15	0.18	0.23	Ref. 112

Finally, we compare the performance of qsGW@RPA and qs Σ^{BSE} @ L^{BSE} against other *GW* approaches. MADs obtained with different methods are collected in table 1. Knight et al.²² have benchmarked the performance of several *GW* methods for the ACC24 set and found G_0W_0 @LRC- ω PBE to perform best, with MADs of 0.13 eV for IPs, and 0.18 eV for EAs. This is very much comparable to our current qsGW@RPA results which shows that qsGW can compete in accuracy with the best one-shot G_0W_0 methods. In Ref. 26, MADs of 0.09 eV for the IPs, 0.07 eV for the EAs and 0.14 eV for the fundamental gaps have been reported using G_0W_0 with the optimally-tuned range-separated hybrid (OTRSH) strategy of Ref. 25 (G_0W_0 @OTRSH). Similar accuracy is achieved for differently tuned G_0W_0 @OTRSH functionals.¹¹⁰ One should notice that G_0W_0 @OTRSH can also be understood as a self-consistent *GW* approach since multiple G_0W_0 calculations have to be performed for different range-separation parameters until the G_0W_0 correction vanishes. It is also worth pointing out that the tuning procedure applied in these works might become problematic for molecules much larger than the ones studied here.¹¹⁰ qs Σ^{BSE} @ L^{BSE} performs equally well for EAs and fundamental gaps. Even though its performance for IPs is worse, it still outperforms most *GW*-based methods. qs Σ^{BSE} @ L^{BSE} also outperforms third-order algebraic diagrammatic construction [ADC(3)]¹¹³, for which MADs of 0.12 eV for IPs and 0.16 eV for EAs have been reported for the same set.¹¹¹

3.2 Neutral excitations

We next calculate the neutral CT excitation energies of the larger molecules in the QUEST #6 database.⁷⁰ We focus here on QUEST #6 since the systems in this database are similar to the ones in ACC24. For instance, Nitrobenzene, Benzonitrile, and Azulene are part of both databases. We therefore can assess whether the accuracy of $\text{qs}\Sigma^{BSE}@L^{BSE}$ for fundamental gaps carries over to neutral excitations.

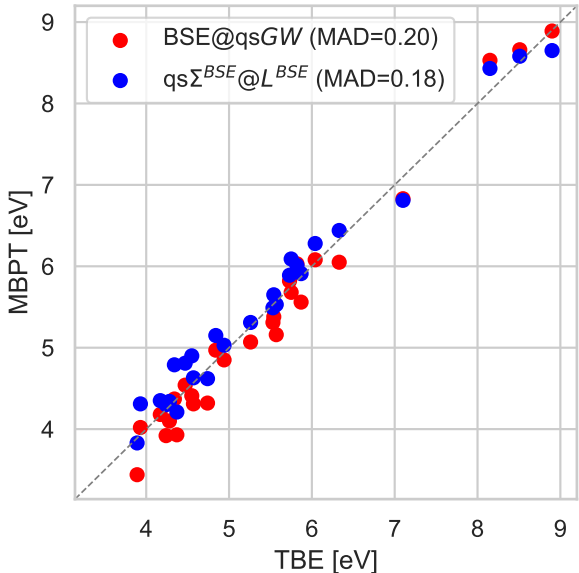


Figure 5: Comparison of neutral charge-transfer excitations in eV for the QUEST # 6 database calculated with BSE@qsGW and $\text{qs}\Sigma^{BSE}@L^{BSE}$ against theoretical best estimates (TBE).⁷⁰

In Fig. 5, we compare the CT excitation energies obtained with qsGW and $\text{qs}\Sigma^{BSE}@L^{BSE}$ against the theoretical best estimates (TBE) of Loos et al.⁷⁰ As expected, the excitation energies strongly correlate with the fundamental QP gap. The wider gap of $\text{qs}\Sigma^{BSE}@L^{BSE}$ with respect to qsGW also results in higher CT excitation energies. Only for the A'' excitations in β -dipeptide and dipeptide, $\text{qs}\Sigma^{BSE}@L^{BSE}$ gives lower excitation energies than qsGW. In both cases, the $\text{qs}\Sigma^{BSE}@L^{BSE}$ fundamental gap is also lower than the qsGW.

For the QUEST #6 database, the BSE@qsGW and $\text{qs}\Sigma^{BSE}@L^{BSE}$ neutral excitations are of the same quality as the ones calculated by Loos et al.⁷⁰ using BSE@evGW@PBE0. Loos et al.⁷⁰ have also benchmarked the accuracy of TD-DFT with different range-separated hybrid functionals and

found them to perform slightly better than BSE@*GW* on average for this particular class of systems. One should notice, that this good performance was only attained by two functionals (CAM-B3LYP¹¹⁴ and ω B97X-D¹¹⁵), while two other functionals (ω B97X¹¹⁶ and LRC- ω HPBE¹¹⁷) perform much worse.⁷⁰ A similar observation was for instance made in Ref. 59. Since it is not clear a priori which functional will perform best for what system, this is a clear disadvantage of TD-DFT@RSH compared to BSE@*GW*. We however also mention that there exist approaches to non-empirically tune the range-separation parameter in RSHs^{118–121} which alleviate this issue a bit.

The observation that $\text{qs}\Sigma^{BSE}@L^{BSE}$ does not outperform BSE@*qsGW* is not unexpected. The former method does not introduce any new diagrams in the BSE. $\text{qs}\Sigma^{BSE}@L^{BSE}$ does only provide different screening and different QP energies, but the QP differences, the quantity entering excited state calculations, are of similar quality. To improve over BSE@*GW*, one likely has to go beyond the first-order vertex in the BSE, as has already been attempted by some authors.^{122–124}

4 Conclusions

We have implemented and tested the $\Sigma^{BSE}@L^{BSE}$ self-energy in a quasi-particle self-consistent framework.^{13,14,36,37} $\Sigma^{BSE}@L^{BSE}$ goes beyond *GW* by adding statically screened particle-hole ladders to the response function *L* and the self-energy, going beyond (diagrammatic) approaches that solve the BSE for *L* but do not add vertex corrections to Σ directly.^{47,125} Adding vertex corrections to *L* only leads to a disastrous performance for molecular EAs and even worse fundamental gaps. Vertex corrections in Σ are needed to cancel the strong electron-hole attraction induced through the vertex in *L*. While vertex corrections in *L* and Σ largely cancel, they increase LUMO energies significantly, and therefore open the fundamental gap. While this leads to a slight overestimation of the gap compared to $\Delta\text{CCSD(T)}$, the performance of $\text{qs}\Sigma^{BSE}@L^{BSE}$ is excellent. It retains the great accuracy of *qsGW* for fundamental gaps and IPs, but greatly improves the EAs. These observations agree with Ref. 65, where the non-screened version of the present self-energy approx-

imation was benchmarked with a HF starting point. An advantage of $\text{qs}\Sigma^{BSE}@L^{BSE}$ over qsGW is its faster convergence to the CBS limit which will be important in practice. We have also assessed $\text{qs}\Sigma^{BSE}@L^{BSE}$ for neutral CT excitations, and found it to perform similarly to qsGW .

The $\Sigma^{BSE}@L^{BSE}$ self-energy has only been introduced very recently.^{59,68,69} Its performance is similar to the self-energy obtained by replacing the statically screened terms with unscreened ones.^{59,63–65,67} In both approximations, the very same vertex is consistently added to L and Σ , which is important for systematic improvements beyond GW .^{26,59} Using the screened interaction instead, as commonly done in $BSE@GW$ calculations,⁷ becomes important for larger molecules.⁵⁹ These recently introduced self-energy approximations are an important step toward robust and diagrammatically motivated approximations to the self-energy beyond the GWA.

At this stage, we see numerous promising avenues for future research that we hope will be pursued soon. Going beyond the quasi-particle approximation and introducing the $\Sigma^{BSE}@L^{BSE}$ self-energy in molecular scGW calculations would be a logical extension of the current work. Due to the relatively strong QP renormalization in solids, it is often claimed that scGW calculations should always be combined with vertex corrections.^{14,19} Using scGW calculations in small atoms and molecules where screening effects are weaker seems to be well justified from a theoretical perspective.^{14,126,127} While scGW calculations are rarely performed and few implementations for molecules exist,^{128–133} very recently Zgid and coworkers reported good agreement with experimental ionization potentials for the GW27 and the SOC81 sets of molecular ionization potentials.^{82,132,134} It would be worthwhile to investigate whether scGW calculations can be systematically improved with vertex corrections, as has been done for solids.^{17,50}

The inclusion of dynamical vertex effects would be another possible extension of this work. Kutepov could show that including the dynamical vertex in L and Σ closes the scGW band gaps, while the static vertex opens them further.¹⁷ The challenge with dynamical vertices lies in the fact that the BSE eq. (2) does not admit a closed-form expression as the L on the left exhibits a different frequency dependence from the L on the right. Consequently, the equation can no longer be solved through diagonalization.^{84,135} Kuwahara, Noguchi, and Ohno¹³⁶ have combined

the dynamical first-order vertex correction to the RPA polarizability with the dynamical $G3W2$ self-energy. While this scheme uses consistent vertices, the first-order vertex corrections in L and Σ cancel almost completely^{59,137,138} and therefore only little improvement over $qsGW$ can be expected. Kutepov went beyond first-order in the dynamical vertex and used an iterative procedure to sum the dynamical BSE eq. (2) order-by-order.¹⁷ One can also think of schemes where the first-order dynamical vertex corrections of Kuwahara et al.¹³⁶ are combined with the infinite-order static correction both for Σ and L .

Vertex corrections beyond the first order. would be another extension of this work. Monino and Loos¹²⁴ and Yamada *et. al.*^{122,123} have found second-order vertex diagrams to change $BSE@GW$ neutral excitation energies significantly. These studies considered only the two of the six second-order vertex diagrams which arise from the variation of W with respect to G . It remains an open question whether further cancellations occur among all six diagrams. It is also not known if the second-order vertex diagrams in Σ and L compensate in the same way as the 1st-order diagrams beyond GW .^{59,137–139} Higher-order vertex corrections Have been investigated by Mejuto-Zaera and Vlček¹⁴⁰ for the Hubbard dimer, and there also exists a recent proposal along these lines by Cunningham.¹²⁵ Implementing and testing such higher-order corrections for molecules would be important to improve the quality of neutral excitation energies. Second-order diagrams in the kernel beyond the ones arising from the variation of W with respect to G could potentially improve triplet excitations, which are only badly described with $BSE@GW$.¹⁴¹

Acknowledgement

The author acknowledges supercomputer facilities at SURFsara sponsored by NWO Physical Sciences, with financial support from The Netherlands Organization for Scientific Research (NWO) and fruitful discussions with Fabien Bruneval.

Supporting Information Available

Detailed derivations and discussions of all equations, additional computational details, and all QP energies calculated in this work,

References

- (1) Hedin, L. New method for calculating the one-particle Green's function with application to the electron-gas problem. *Phys. Rev.* **1965**, *139*, A796.
- (2) Strinati, G. Application of the Green's functions method to the study of the optical properties of semiconductors. *La Riv. Del Nuovo Cim. Ser. 3* **1988**, *11*, 1–86.
- (3) Aryasetiawan, F.; Gunnarsson, O. The GW method. *Reports Prog. Phys.* **1998**, *61*, 237–312.
- (4) Fetter, A. L.; Walecka, J. D. *Quantum theory of many-particle systems*; Dover Publications INC. New York, 2003.
- (5) Martin, R. M.; Reining, L.; Ceperley, D. M. *Interacting electrons*; Cambridge University Press, 2016.
- (6) Reining, L. The GW approximation: content, successes and limitations. *Wiley Interdiscip. Rev. Comput. Mol. Sci.* **2018**, *8*, e1344.
- (7) Blase, X.; Duchemin, I.; Jacquemin, D. The Bethe–Salpeter equation in chemistry: Relations with TD-DFT, applications and challenges. *Chem. Soc. Rev.* **2018**, *47*, 1022–1043.
- (8) Golze, D.; Dvorak, M.; Rinke, P. The GW Compendium: A Practical Guide to Theoretical Photoemission Spectroscopy. *Front. Chem.* **2019**, *7*, 377.
- (9) Marie, A.; Ammar, A.; Loos, P. F. The GW approximation: A quantum chemistry perspective. *Adv. Quantum Chem.* **2024**,

- (10) Gell-Mann, M.; Brueckner, K. A. Correlation energy of an electron gas at high density. *Phys. Rev.* **1957**, *106*, 364–368.
- (11) Macke, W. Über die Wechselwirkungen im Fermi-Gas. *Zeitschrift für Naturforsch.* **1950**, *5*, 192–208.
- (12) Nozières, P.; Pines, D. Correlation energy of a free electron gas. *Phys. Rev.* **1958**, *111*, 442–454.
- (13) Faleev, S. V.; van Schilfgaarde, M.; Kotani, T. All-electron self-consistent GW approximation: Application to Si, MnO, and NiO. *Phys. Rev. Lett.* **2004**, *93*, 126406.
- (14) Bruneval, F.; Gatti, M. In *First Principles Approaches to Spectroscopic Properties of Complex Materials*; Di Valentin, C., Botti, S., Cococcioni, M., Eds.; Topics in Current Chemistry; Springer Berlin Heidelberg, 2014; Vol. 347; pp 99–136.
- (15) Holm, B.; von Barth, U. Fully self-consistent self-energy of the electron gas. *Phys. Rev. B - Condens. Matter Mater. Phys.* **1998**, *57*, 2108–2117.
- (16) Kutepov, A.; Haule, K.; Savrasov, S. Y.; Kotliar, G. Electronic structure of Pu and Am metals by self-consistent relativistic GW method. *Phys. Rev. B - Condens. Matter Mater. Phys.* **2012**, *85*, 155129.
- (17) Kutepov, A. L. Electronic structure of Na, K, Si, and LiF from self-consistent solution of Hedin’s equations including vertex corrections. *Phys. Rev. B* **2016**, *94*, 155101.
- (18) Grumet, M.; Liu, P.; Kaltak, M.; Klimeš, J.; Kresse, G. Beyond the quasiparticle approximation: Fully self-consistent GW calculations. *Phys. Rev. B* **2018**, *98*, 155143.
- (19) Rohlfing, M. Approximate spatiotemporal structure of the vertex function $\Gamma(1, 2;3)$ in many-body perturbation theory. *Phys. Rev. B* **2023**, *108*, 195207.
- (20) Kohn, W.; Sham, L. J. Self-Consistent Equations Including Exchange and Correlation Effects. *Phys. Rev.* **1965**, *140*, A1133.

- (21) Hybertsen, M. S.; Louie, S. G. First-principles theory of quasiparticles: Calculation of band gaps in semiconductors and insulators. *Phys. Rev. Lett.* **1985**, *55*, 1418–1421.
- (22) Knight, J. W.; Wang, X.; Gallandi, L.; Dolgounitcheva, O.; Ren, X.; Ortiz, J. V.; Rinke, P.; Körzdörfer, T.; Marom, N. Accurate Ionization Potentials and Electron Affinities of Acceptor Molecules III: A Benchmark of GW Methods. *J. Chem. Theory Comput.* **2016**, *12*, 615–626.
- (23) Caruso, F.; Dauth, M.; Van Setten, M. J.; Rinke, P. Benchmark of GW Approaches for the GW100 Test Set. *J. Chem. Theory Comput.* **2016**, *12*, 5076–5087.
- (24) Bruneval, F.; Dattani, N.; van Setten, M. J. The GW Miracle in Many-Body Perturbation Theory for the Ionization Potential of Molecules. *Front. Chem.* **2021**, *9*, 749779.
- (25) McKeon, C. A.; Hamed, S. M.; Bruneval, F.; Neaton, J. B. An optimally tuned range-separated hybrid starting point for ab initio GW plus Bethe-Salpeter equation calculations of molecules. *J. Chem. Phys.* **2022**, *157*, 074103.
- (26) Bruneval, F.; Förster, A. Fully dynamic G3W2 self-energy for finite systems: Formulas and benchmark. *J. Chem. Theory Comput.* **2024**, *20*, 3218–3230.
- (27) Golze, D.; Keller, L.; Rinke, P. Accurate Absolute and Relative Core-Level Binding Energies From GW. *J. Phys. Chem. Lett.* **2020**, *11*, 1840–1847.
- (28) Li, J.; Jin, Y.; Rinke, P.; Yang, W.; Golze, D. Benchmark of GW Methods for Core-Level Binding Energies. *J. Chem. Theory Comput.* **2022**, *18*, 7570–7585.
- (29) Blase, X.; Attaccalite, C.; Olevano, V. First-principles GW calculations for fullerenes, porphyrins, phthalocyanine, and other molecules of interest for organic photovoltaic applications. *Phys. Rev. B* **2011**, *83*, 115103.
- (30) Faber, C.; Attaccalite, C.; Olevano, V.; Runge, E.; Blase, X. First-principles GW calculations for DNA and RNA nucleobases. *Phys. Rev. B* **2011**, *81*, 115123.

- (31) Bruneval, F.; Marques, M. Benchmarking the starting points of the GW approximation for molecules. *J. Chem. Theory Comput.* **2013**, *9*, 324–329.
- (32) Bruneval, F. Improved density matrices for accurate molecular ionization potentials. *Phys. Rev. B* **2019**, *99*, 041118(R).
- (33) Onida, G.; Reining, L.; Rubio, A. Electronic excitations: density-functional versus many-body Green's-function approaches. *Rev. Mod. Phys.* **2002**, *74*, 601.
- (34) Förster, A.; Visscher, L. Quasiparticle Self-Consistent GW-Bethe-Salpeter equation calculations for large chromophoric systems. *J. Chem. Theory Comput.* **2022**, *18*, 6779–6793.
- (35) Kshirsagar, A. R.; Poloni, R. Assessing the Role of the Kohn-Sham Density in the Calculation of the Low-Lying Bethe-Salpeter Excitation Energies. *J. Phys. Chem. A* **2023**, *127*, 2618–2627.
- (36) van Schilfgaarde, M.; Kotani, T.; Faleev, S. Quasiparticle self-consistent GW theory. *Phys. Rev. Lett.* **2006**, *96*, 226402.
- (37) Kotani, T.; van Schilfgaarde, M.; Faleev, S. V. Quasiparticle self-consistent GW method: A basis for the independent-particle approximation. *Phys. Rev. B* **2007**, *76*, 165106.
- (38) Similar to other electronic structure methods, for instance, Hartree–Fock (HF) theory, there can of course be multiple solutions corresponding to different local minima which may be reached from different starting points.
- (39) Förster, A.; Visscher, L. Low-Order Scaling Quasiparticle Self-Consistent GW for Molecules. *Front. Chem.* **2021**, *9*, 736591.
- (40) Gui, X.; Holzer, C.; Klopper, W. Accuracy Assessment of GW Starting Points for Calculating Molecular Excitation Energies Using the Bethe-Salpeter Formalism. *J. Chem. Theory Comput.* **2018**, *14*, 2127–2136.

- (41) Förster, A.; Visscher, L. Exploring the statically screened G3W2 correction to the GW self-energy : Charged excitations and total energies of finite systems. *Phys. Rev. B* **2022**, *105*, 125121.
- (42) Shishkin, M.; Marsman, M.; Kresse, G. Accurate quasiparticle spectra from self-consistent GW calculations with vertex corrections. *Phys. Rev. Lett.* **2007**, *99*, 246403.
- (43) Bruneval, F.; Vast, N.; Reining, L.; Izquierdo, M.; Sirotti, F.; Barrett, N. Exchange and correlation effects in electronic excitations of Cu2O. *Phys. Rev. Lett.* **2006**, *97*, 267601.
- (44) Chen, W.; Pasquarello, A. Accurate band gaps of extended systems via efficient vertex corrections in GW. *Phys. Rev. B - Condens. Matter Mater. Phys.* **2015**, *92*, 041115(R).
- (45) Tal, A.; Chen, W.; Pasquarello, A. Vertex function compliant with the Ward identity for quasiparticle self-consistent calculations beyond GW. *Phys. Rev. B* **2021**, *103*, 161104.
- (46) Cunningham, B.; Grüning, M.; Pashov, D.; Van Schilfgaarde, M. QSG \hat{W} : Quasiparticle self-consistent GW with ladder diagrams in W. *Phys. Rev. B* **2023**, *108*, 165104.
- (47) Cunningham, B.; Grüning, M.; Azarhoosh, P.; Pashov, D.; van Schilfgaarde, M. Effect of ladder diagrams on optical absorption spectra in a quasiparticle self-consistent GW framework. *Phys. Rev. Mater.* **2018**, *2*, 034603.
- (48) Grüneis, A.; Kresse, G.; Hinuma, Y.; Oba, F. Ionization potentials of solids: The importance of vertex corrections. *Phys. Rev. Lett.* **2014**, *112*, 096401.
- (49) Kuwahara, R.; Ohno, K. Linearized self-consistent GW approach satisfying the Ward identity. *Phys. Rev. A - At. Mol. Opt. Phys.* **2014**, *90*, 032506.
- (50) Kutepov, A. L.; Kotliar, G. One-electron spectra and susceptibilities of the three-dimensional electron gas from self-consistent solutions of Hedin's equations. *Phys. Rev. B* **2017**, *96*, 035108.

- (51) Abdallah, M. S.; Pasquarello, A. Quasiparticle self-consistent GW with effective vertex corrections in the polarizability and the self-energy applied to MnO, FeO, CoO, and NiO. *Phys. Rev. B* **2024**, *110*, 155105.
- (52) Bruneval, F. Ionization energy of atoms obtained from GW self-energy or from random phase approximation total energies. *J. Chem. Phys.* **2012**, *136*, 194107.
- (53) Ke, S. H. All-electron GW methods implemented in molecular orbital space: Ionization energy and electron affinity of conjugated molecules. *Phys. Rev. B* **2011**, *84*, 205415.
- (54) Kaplan, F.; Harding, M. E.; Seiler, C.; Weigend, F.; Evers, F.; Van Setten, M. J. Quasi-Particle Self-Consistent GW for Molecules. *J. Chem. Theory Comput.* **2016**, *12*, 2528–2541.
- (55) Marie, A.; Loos, P.-F. A Similarity Renormalization Group Approach to Green's Function Methods. *J. Chem. Theory Comput.* **2023**, *19*, 3943-3957.
- (56) Marie, A.; Loos, P. F. Reference Energies for Valence Ionizations and Satellite Transitions. *J. Chem. Theory Comput.* **2024**, *20*, 4751–4777.
- (57) Purvis, G. D.; Bartlett, R. J. A full coupled-cluster singles and doubles model: The inclusion of disconnected triples. *J. Chem. Phys.* **1982**, *76*, 1910–1918.
- (58) Lewis, A. M.; Berkelbach, T. C. Vertex Corrections to the Polarizability Do Not Improve the GW Approximation for the Ionization Potential of Molecules. *J. Chem. Theory Comput.* **2019**, *15*, 2925–2932.
- (59) Förster, A.; Bruneval, F. Why does the \$GW\$ approximation give accurate quasiparticle energies? The cancellation of vertex corrections quantified. *arXiv:2410.17843* **2024**, 1–8.
- (60) Förster, A.; van Lenthe, E.; Spadetto, E.; Visscher, L. Two-component \$GW\$ calculations: Cubic scaling implementation and comparison of partially self-consistent variants. *J. Chem. Theory Comput.* **2023**, *19*, 5958–5976.

- (61) Ren, X.; Marom, N.; Caruso, F.; Scheffler, M.; Rinke, P. Beyond the GW approximation: A second-order screened exchange correction. *Phys. Rev. B - Condens. Matter Mater. Phys.* **2015**, *92*, 081104(R).
- (62) Wang, Y.; Rinke, P.; Ren, X. Assessing the G₀W₀Γ₀(1) Approach: Beyond G₀W₀ with Hedin's Full Second-Order Self-Energy Contribution. *J. Chem. Theory Comput.* **2021**, *17*, 5140–5154.
- (63) Maggio, E.; Kresse, G. GW Vertex Corrected Calculations for Molecular Systems. *J. Chem. Theory Comput.* **2017**, *13*, 4765–4778.
- (64) Maggio, E.; Kresse, G. Correction to: GW Vertex corrected calculations for molecular systems. *J. Chem. Theory Comput.* **2018**, *14*, 1821.
- (65) Vlček, V. Stochastic Vertex Corrections: Linear Scaling Methods for Accurate Quasiparticle Energies. *J. Chem. Theory Comput.* **2019**, *15*, 6254–6266.
- (66) Mejuto-Zaera, C.; Weng, G.; Romanova, M.; Cotton, S. J.; Whaley, K. B.; Tubman, N. M.; Vlček, V. Are multi-quasiparticle interactions important in molecular ionization? *J. Chem. Phys.* **2021**, *154*, 121101.
- (67) Vacondio, S.; Varsano, D.; Ruini, A.; Ferretti, A. Going Beyond the GW Approximation Using the Time-Dependent Hartree-Fock Vertex. *J. Chem. Theory Comput.* **2024**, *20*, 4718–4737.
- (68) Patterson, C. H. Molecular Ionization Energies from GW and Hartree-Fock Theory: Polarizability, Screening, and Self-Energy Vertex Corrections. *J. Chem. Theory Comput.* **2024**, *20*, 7479–7493.
- (69) Patterson, C. H. Erratum: Molecular Ionization Energies from GW and Hartree-Fock Theory: Polarizability, Screening and Self-Energy Vertex Corrections. *J. Chem. Theory Comput.* **2024**, *20*, 9267.

- (70) Loos, P. F.; Comin, M.; Blase, X.; Jacquemin, D. Reference Energies for Intramolecular Charge-Transfer Excitations. *J. Chem. Theory Comput.* **2021**, *17*, 3666–3686.
- (71) Loos, P. F.; Scemama, A.; Blondel, A.; Garniron, Y.; Caffarel, M.; Jacquemin, D. A Mountaineering Strategy to Excited States: Highly Accurate Reference Energies and Benchmarks. *J. Chem. Theory Comput.* **2018**, *14*, 4360–4379.
- (72) Loos, P. F.; Scemama, A.; Jacquemin, D. The Quest for Highly Accurate Excitation Energies: A Computational Perspective. *J. Phys. Chem. Lett.* **2020**, *11*, 2374–2383.
- (73) Véril, M.; Scemama, A.; Caffarel, M.; Lipparini, F.; Boggio-Pasqua, M.; Jacquemin, D.; Loos, P. F. QUESTDB: A database of highly accurate excitation energies for the electronic structure community. *Wiley Interdiscip. Rev. Comput. Mol. Sci.* **2021**, *11*, e1517.
- (74) Baym, G.; Kadanoff, L. P. Conservation laws and correlation functions. *Phys. Rev.* **1961**, *124*, 287–299.
- (75) Romaniello, P.; Bechstedt, F.; Reining, L. Beyond the GW approximation: Combining correlation channels. *Phys. Rev. B* **2012**, *85*, 155131.
- (76) Orlando, R.; Romaniello, P.; Loos, P. F. The three channels of many-body perturbation theory: GW, particle-particle, and electron-hole T-matrix self-energies. *J. Chem. Phys.* **2023**, *159*, 184113.
- (77) Starke, R.; Kresse, G. Self-consistent Green function equations and the hierarchy of approximations for the four-point propagator. *Phys. Rev. B* **2012**, *85*, 075119.
- (78) Sakuma, R.; Miyake, T.; Aryasetiawan, F. Effective quasiparticle Hamiltonian based on Löwdin’s orthogonalization. *Phys. Rev. B - Condens. Matter Mater. Phys.* **2009**, *80*, 235128.
- (79) Kutepov, A. L.; Oudovenko, V. S.; Kotliar, G. Linearized self-consistent quasiparticle GW method: Application to semiconductors and simple metals. *Comput. Phys. Commun.* **2017**, *219*, 407–414.

- (80) Ismail-Beigi, S. Justifying quasiparticle self-consistent schemes via gradient optimization in Baym-Kadanoff theory. *J. Phys. Condens. Matter* **2017**, *29*, 385501.
- (81) Lei, J.; Zhu, T. Gaussian-based quasiparticle self-consistent GW for periodic systems. *J. Chem. Phys.* **2022**, *157*, 214114.
- (82) Harsha, G.; Abraham, V.; Wen, M.; Zgid, D. Quasiparticle and fully self-consistent GW methods: an unbiased analysis using Gaussian orbitals. *arXiv:2406.18077* **2024**, 61–66.
- (83) Sander, T.; Maggio, E.; Kresse, G. Beyond the Tamm-Dancoff approximation for extended systems using exact diagonalization. *Phys. Rev. B - Condens. Matter Mater. Phys.* **2015**, *92*, 045209.
- (84) Romaniello, P.; Sangalli, D.; Berger, J. A.; Sottile, F.; Molinari, L. G.; Reining, L.; Onida, G. Double excitations in finite systems. *J. Chem. Phys.* **2009**, *130*, 044108.
- (85) Acharya, S.; Pashov, D.; Cunningham, B.; Rudenko, A. N.; Rösner, M.; Grüning, M.; van Schilfgaarde, M.; Katsnelson, M. I. Electronic Structure of Chromium Trihalides beyond Density Functional Theory. *Phys. Rev. B* **2021**, *104*, 155109.
- (86) Acharya, S.; Pashov, D.; Rudenko, A. N.; Rösner, M.; van Schilfgaarde, M.; Katsnelson, M. I. Importance of charge self-consistency in first-principles description of strongly correlated systems. *npj Comput. Mater.* **2021**, *7*, 208.
- (87) Radha, S. K.; Lambrecht, W.; Cunningham, B.; Grüning, M.; Pashov, D.; van Schilfgaarde, M. Optical response and band structure of LiCoO₂ including electron-hole interaction effects. *Phys. Rev. B* **2021**, *104*, 115120.
- (88) Dadkhah, N.; Lambrecht, W. R.; Pashov, D.; Van Schilfgaarde, M. Improved quasiparticle self-consistent electronic band structure and excitons in β -LiGaO₂. *Phys. Rev. B* **2023**, *107*, 165201.

- (89) Garcia, C.; Radha, S. K.; Acharya, S.; Lambrecht, W. R. Quasiparticle band structure and excitonic optical response in V2 O5 bulk and monolayer. *Phys. Rev. B* **2024**, *110*, 85102.
- (90) Hirata, S.; Head-Gordon, M. Time-dependent density functional theory within the Tamm-Dancoff approximation. *Chem. Phys. Lett.* **1999**, *314*, 291–299.
- (91) Kutepov, A. L. Full versus quasiparticle self-consistency in vertex-corrected GW approaches. *Phys. Rev. B* **2022**, *105*, 045124.
- (92) Te Velde, G.; Baerends, E. J. Precise density-functional method for periodic structures. *Phys. Rev. B* **1991**, *44*, 7888–7903.
- (93) Bruneval, F.; Rangel, T.; Hamed, S. M.; Shao, M.; Yang, C.; Neaton, J. B. MOLGW 1: Many-body perturbation theory software for atoms, molecules, and clusters. *Comput. Phys. Commun.* **2016**, *208*, 149–161.
- (94) Dunning, T. H. Gaussian basis sets for use in correlated molecular calculations. I. The atoms boron through neon and hydrogen. *J. Chem. Phys.* **1989**, *90*, 1007–1023.
- (95) Kendall, R. A.; Dunning, T. H.; Harrison, R. J. Electron affinities of the first-row atoms revisited. Systematic basis sets and wave functions. *J. Chem. Phys.* **1992**, *96*, 6796–6806.
- (96) Spadetto, E.; Philipson, P. H. T.; Förster, A.; Visscher, L. Toward Pair Atomic Density Fitting for Correlation Energies with Benchmark Accuracy. *J. Chem. Theory Comput.* **2023**, *19*, 1499–1516.
- (97) te Velde, G.; Bickelhaupt, F. M.; Baerends, E. J.; Fonseca Guerra, C.; van Gisbergen, S.; Snijders, J. G.; Ziegler, T. Chemistry with ADF. *J. Comput. Chem.* **2001**, *22*, 931–967.
- (98) Van Lenthe, E.; Baerends, J. E. Optimized Slater-type basis sets for the elements 1–118. *J. Comput. Chem.* **2003**, *24*, 1142–1156.
- (99) Förster, A.; Visscher, L. GW100: A Slater-Type Orbital Perspective. *J. Chem. Theory Comput.* **2021**, *17*, 5080–5097.

- (100) Pulay, P. Convergence acceleration of iterative sequences. The case of scf iteration. *Chem. Phys. Lett.* **1980**, *73*, 393–398.
- (101) Véril, M.; Romaniello, P.; Berger, J. A.; Loos, P. F. Unphysical Discontinuities in GW Methods. *J. Chem. Theory Comput.* **2018**, *14*, 5220–5228.
- (102) Bruneval, F.; Maliyov, I.; Lapointe, C.; Marinica, M.-C. Extrapolating unconverged GW energies up to the complete basis set limit with linear regression. *J. Chem. Theory Comput.* **2020**, *16*, 4399–4407.
- (103) Monkhorst, H. J. Calculation of properties with the coupled-cluster method. *Int. J. Quantum Chem.* **1977**, *12*, 421–432.
- (104) Koch, H.; Jørgensen, P. Coupled cluster response functions. *J. Chem. Phys.* **1990**, *93*, 3333–3344.
- (105) Stanton, J. F.; Bartlett, R. J. The equation of motion coupled-cluster method. A systematic biorthogonal approach to molecular excitation energies, transition probabilities, and excited state properties. *J. Chem. Phys.* **1993**, *98*, 7029–7039.
- (106) Stuke, A.; Kunkel, C.; Golze, D.; Todorović, M.; Margraf, J. T.; Reuter, K.; Rinke, P.; Oberhofer, H. Atomic structures and orbital energies of 61,489 crystal-forming organic molecules. *Sci. Data* **2020**, *7*, 1–11.
- (107) Jensen, F. Atomic orbital basis sets. *Wiley Interdiscip. Rev. Comput. Mol. Sci.* **2013**, *3*, 273–295.
- (108) Richard, R. M.; Marshall, M. S.; Dolgounitcheva, O.; Ortiz, J. V.; Brédas, J. L.; Marom, N.; Sherrill, C. D. Accurate Ionization Potentials and Electron Affinities of Acceptor Molecules I. Reference Data at the CCSD(T) Complete Basis Set Limit. *J. Chem. Theory Comput.* **2016**, *12*, 595–604.

- (109) Irmeler, A.; Grüneis, A. Particle-particle ladder based basis-set corrections applied to atoms and molecules using coupled-cluster theory. *J. Chem. Phys.* **2019**, *151*, 104107.
- (110) Gallandi, L.; Marom, N.; Rinke, P.; Körzdörfer, T. Accurate Ionization Potentials and Electron Affinities of Acceptor Molecules II: Non-Empirically Tuned Long-Range Corrected Hybrid Functionals. *J. Chem. Theory Comput.* **2016**, *12*, 605–614.
- (111) Dolgounitcheva, O.; Díaz-Tinoco, M.; Zakrzewski, V. G.; Richard, R. M.; Marom, N.; Sherrill, C. D.; Ortiz, J. V. Accurate Ionization Potentials and Electron Affinities of Acceptor Molecules IV: Electron-Propagator Methods. *J. Chem. Theory Comput.* **2016**, *12*, 627–637.
- (112) Fürst, S.; Kaupp, M. Accurate Ionization Potentials, Electron Affinities, and Band Gaps from the ω LH22t Range-Separated Local Hybrid Functional: No Tuning Required. *J. Chem. Theory Comput.* **2023**, *19*, 3146–3158.
- (113) von Niessen, W.; Schirmer, J.; Cederbaum, L. S. Computational Methods For The One-Particle Green's Function. *Comput. Phys. Reports* **1984**, *1*, 57-125.
- (114) Yanai, T.; Tew, D. P.; Handy, N. C. A new hybrid exchange-correlation functional using the Coulomb-attenuating method (CAM-B3LYP). *Chem. Phys. Lett.* **2004**, *393*, 51–57.
- (115) Chai, J. D.; Head-Gordon, M. Long-range corrected hybrid density functionals with damped atom-atom dispersion corrections. *Phys. Chem. Chem. Phys.* **2008**, *10*, 6615–6620.
- (116) Chai, J. D.; Head-Gordon, M. Systematic optimization of long-range corrected hybrid density functionals. *J. Chem. Phys.* **2008**, *128*, 084106.
- (117) Rohrdanz, M. A.; Martins, K. M.; Herbert, J. M. A long-range-corrected density functional that performs well for both ground-state properties and time-dependent density functional theory excitation energies, including charge-transfer excited states. *J. Chem. Phys.* **2009**, *130*, 054112.

- (118) Stein, T.; Eisenberg, H.; Kronik, L.; Baer, R. Fundamental gaps in finite systems from eigenvalues of a generalized Kohn-Sham method. *Phys. Rev. Lett.* **2010**, *105*, 266802.
- (119) Refaely-Abramson, S.; Baer, R.; Kronik, L. Fundamental and excitation gaps in molecules of relevance for organic photovoltaics from an optimally tuned range-separated hybrid functional. *Phys. Rev. B - Condens. Matter Mater. Phys.* **2011**, *84*, 075144.
- (120) Refaely-Abramson, S.; Sharifzadeh, S.; Govind, N.; Autschbach, J.; Neaton, J. B.; Baer, R.; Kronik, L. Quasiparticle spectra from a nonempirical optimally tuned range-separated hybrid density functional. *Phys. Rev. Lett.* **2012**, *109*, 226405.
- (121) Kronik, L.; Stein, T.; Refaely-Abramson, S.; Baer, R. Excitation gaps of finite-sized systems from optimally tuned range-separated hybrid functionals. *J. Chem. Theory Comput.* **2012**, *8*, 1515–1531.
- (122) Yamada, S.; Noguchi, Y.; Ishii, K.; Hirose, D.; Sugino, O.; Ohno, K. Development of the Bethe-Salpeter method considering second-order corrections for a GW electron-hole interaction kernel. *Phys. Rev. B* **2022**, *106*, 045113.
- (123) Yamada, S.; Noguchi, Y. Significant contributions of second-order exchange terms in GW electron-hole interaction kernel for charge-transfer excitations. *J. Chem. Phys.* **2023**, *159*, 234105.
- (124) Monino, E.; Loos, P.-f. Connections and performances of Green's function methods for charged and neutral excitations. *J. Chem. Phys.* **2023**, *159*, 034105.
- (125) Cunningham, B. Many body theory beyond GW : towards a complete description of 2-body correlated propagation. *Arxiv:2411.03958* **2024**, 1–9.
- (126) Stan, A.; Dahlen, N. E.; Van Leeuwen, R. Fully self-consistent GW calculations for atoms and molecules. *Europhys. Lett.* **2006**, *76*, 298–304.

- (127) Stan, A.; Dahlen, N. E.; van Leeuwen, R. Levels of self-consistency in the GW approximation. *J. Chem. Phys.* **2009**, *130*, 114105.
- (128) Rostgaard, C.; Jacobsen, K. W.; Thygesen, K. S. Fully self-consistent GW calculations for molecules. *Phys. Rev. B* **2010**, *81*, 085103.
- (129) Koval, P.; Foerster, D.; Sánchez-Portal, D. Fully self-consistent GW and quasiparticle self-consistent GW for molecules. *Phys. Rev. B* **2014**, *89*, 155417.
- (130) Caruso, F.; Rinke, P.; Ren, X.; Scheffler, M.; Rubio, A. Unified description of ground and excited states of finite systems: The self-consistent GW approach. *Phys. Rev. B* **2012**, *86*, 081102(R).
- (131) Caruso, F.; Rinke, P.; Ren, X.; Rubio, A.; Scheffler, M. Self-consistent GW: All-electron implementation with localized basis functions. *Phys. Rev. B* **2013**, *88*, 075105.
- (132) Abraham, V.; Harsha, G.; Zgid, D. Relativistic Fully Self-Consistent GW for Molecules: Total Energies and Ionization Potentials. *J. Chem. Theory Comput.* **2024**, *20*, 4579–4590.
- (133) Iskakov, S.; Yeh, C.-N.; Pokhilko, P.; Yu, Y.; Zhang, L.; Harsha, G.; Abraham, V.; Wen, M.; Wang, M.; Adamski, J.; Chen, T.; Gull, E.; Zgid, D. Green/WeakCoupling: Implementation of fully self-consistent finite-temperature many-body perturbation theory for molecules and solids. *arXiv:2406.18479* **2024**,
- (134) Scherpelz, P.; Govoni, M.; Hamada, I.; Galli, G. Implementation and Validation of Fully Relativistic GW Calculations: Spin-Orbit Coupling in Molecules, Nanocrystals, and Solids. *J. Chem. Theory Comput.* **2016**, *12*, 3523–3544.
- (135) Sangalli, D.; Romaniello, P.; Onida, G.; Marini, A. Double excitations in correlated systems: A many-body approach. *J. Chem. Phys.* **2011**, *134*, 034115.

- (136) Kuwahara, R.; Noguchi, Y.; Ohno, K. GW Γ + Bethe-Salpeter equation approach for photoabsorption spectra: Importance of self-consistent GW Γ calculations in small atomic systems. *Phys. Rev. B* **2016**, *94*, 121116(R).
- (137) Bobbert, P. A.; Van Haeringen, W. Lowest-order vertex-correction contribution to the direct gap of silicon. *Phys. Rev. B* **1994**, *49*, 10326–10331.
- (138) de Groot, H.; Ummels, R.; Bobbert, P.; Haeringen, W. V. Lowest-order corrections to the RPA polarizability and GW self-energy of a semiconducting wire. *Phys. Rev. B - Condens. Matter Mater. Phys.* **1996**, *54*, 2374–2380.
- (139) Ummels, R.; Bobbert, P. A.; van Haeringen, W. First-order corrections to random-phase approximation calculations in silicon and diamond. *Phys. Rev. B - Condens. Matter Mater. Phys.* **1998**, *57*, 11962–11973.
- (140) Mejuto-Zaera, C.; Vlček, V. Self-consistency in GW Γ formalism leading to quasiparticle-quasiparticle couplings. *Phys. Rev. B* **2022**, *106*, 165129.
- (141) Rangel, T.; Hamed, S. M.; Bruneval, F.; Neaton, J. B. An assessment of low-lying excitation energies and triplet instabilities of organic molecules with an ab initio Bethe-Salpeter equation approach and the Tamm-Dancoff approximation. *J. Chem. Phys.* **2017**, *146*, 194108.

TOC Graphic

